

1  
2  
3  
4  
5  
6  
7  
8  
9  
10  
11  
12  
13  
14  
15  
16  
17  
18  
19  
20  
21  
22  
23

**Revision 1**

**Manuscript 5899**

**Further Observations Related To A Possible Occurrence Of Terrestrial Ahrensite**

William E. Glassley<sup>1,2</sup>, John A. Korstgård<sup>2</sup>, Kai Sørensen<sup>3</sup>

<sup>1</sup>Department of Geology, University of California, Davis, California 95616,  
U.S.A.

<sup>2</sup>Department of Geoscience, Aarhus University, 8000 Århus C, Denmark

<sup>3</sup>Geological Survey of Denmark and Greenland (GEUS), Copenhagen, Denmark

Abstract: Clusters of aligned, highly elongate, prismatic quartz (Qtz) rods occur in a few fayalite (Fa) crystals in a eulysite from a recently identified ~1.8 Gy UHP site in central West Greenland (Glassley et al., 2014). Additional detailed analyses of the crystallography and phase compositions of these olivines were conducted to evaluate the postulate that the Qtz rods formed during inversion of super-silicic ahrensite to Fa+Qtz during decompression. These new observations show the Qtz rods consistently occur in crystallographically coherent clusters with the Qtz grains aligned parallel to [100] of Fa. The contrasting compositions of co-existing primary UHP Fa and Fa postulated to have formed by inversion of ahrensite are consistent with the inversion scenario. We thus conclude that all available data are consistent with the postulate that ahrensite was part of the equilibrium phase assemblage formed during UHP metamorphism and that it inverted

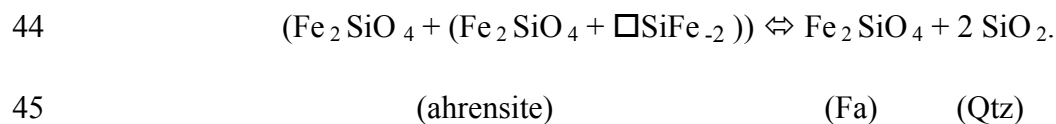
24 to Fa+Qtz upon decompression. If true, this would represent the first occurrence of  
25 terrestrial ahrensite formed through natural tectonic processes.

26

27

## 28 **Introduction**

29 In an earlier paper documenting evidence for a new UHP regime (ca. 6-8 GPa at  
30 ~1,000°C; ~1.8 Gy) in central West Greenland (Glassley et al., 2014), we reported the  
31 occasional occurrence of quartz “lamellae” (for reasons noted below, we will henceforth  
32 refer to these as rods) in fayalitic olivines (Fa) in our sample 123220, an Fe-Mn-rich  
33 olivine-pyroxene-quartz-garnet metasediment (eulysite). Because the rods are prismatic,  
34 clustered in parallel arrays and have a uniform morphology reminiscent of exsolution  
35 features, we postulated they formed as a result of exsolution from the host Fa. Super-  
36 silicic Fa has not been reported in the literature, but excess silica has been reported for  
37 spinel-structured olivines (i.e., the wadsleyite-ringwoodite series) from experimental  
38 studies (Akaogi and Akimoto, 1979; Irifune and Ringwood, 1987; Hazen et al., 1993).  
39 Theoretically, therefore, spinel-structured, super-silicic olivine could exsolve silica upon  
40 decompression and inversion to olivine. On the basis of these experimental results we  
41 therefore postulated that the Qtz rods formed in response to inversion of high-pressure  
42 super-silicic ahrensite (Fe-rich ringwoodite) to Fa during decompression, the reaction  
43 being



46 where excess Si in the ahrensite is accommodated via a vacancy substitution mechanism  
47 in which  $\square\text{SiFe}_2$  (Day and Mulcahy 2007) occurs. If correct, sample 123220 contains  
48 the first known occurrence in which ahrensite resulted from tectonic processes on earth,  
49 rather than shock-induced transformations related to meteorite impacts (Xie et al., 2002;  
50 Feng et al., 2011; Ma et al., 2014, 2016) or anthropogenic activity (Diaz-Martinez and  
51 Ormō, 2003).

52

53 To further document the characteristics of this unusual phase relationship, we report here  
54 the results of additional optical and chemical analyses of this sample. This research  
55 involved a grain-by-grain examination of every olivine crystal in a thin section of sample  
56 123220, and further comparison of the observed olivine compositions with published  
57 experimental data of olivine ( $\alpha$ -phase) and Fe-ringwoodite (i.e., ahrensite;  $\gamma$ -phase).

58

### 59 **Assumptions**

60 If the Qtz rods formed as a result of exsolution, a systematic relationship would be  
61 observed in thin section in which: 1) the crystallographic orientation of the host Fa and  
62 the elongation direction of the rods is consistent; 2) the crystallographic orientation of the  
63 Fa host and the enclosed Qtz rods is consistent (which also requires that all of the rods in  
64 a given host have the same crystallographic orientation); and 3) all of the rods occur  
65 along a low-energy interface such as a primary crystallographic axis. Assuming that the  
66 rods are aligned parallel to one of the principal Fa crystallographic axes, the maximum  
67 elongation of the Qtz rods would be observed when the crystallographic axis of interest  
68 lay in the plane of the thin section. When that same crystallographic axis is oriented

69 perpendicular to the plane of the thin section, the rods would be seen in cross section and  
70 exhibit minimum dimensions. In any other orientation, the maximum rod length would be  
71 some intermediate value, the absolute magnitude of which would depend upon the angle  
72 between the axis of interest and the plane of the thin section. Hence, if the rods result  
73 from exsolution, a sufficiently large number of measurements would exhibit a correlation  
74 between measured rod lengths and the Fa crystallographic orientations. In addition, all  
75 Qtz rods in a given host crystal, and the host crystal itself, would go to extinction at the  
76 same time.

77

78 The advantage of this optical petrography approach is that the abundance, grain geometry  
79 (size and shape) of the original ahrensite, and the rod morphology can all be established  
80 with a single observational technique. A limitation, however, is that the thin section slice  
81 is a random 30  $\mu$  slab through crystals that, in this instance, have much longer observed  
82 lengths. Hence, measurements of rod lengths are most likely to provide minimum values.

83

#### 84 **Optical Observations**

85 Every olivine grain in a thin section of 123220 was surveyed for the presence of quartz  
86 rods using a polarizing microscope. For each Fa grain that contained such clusters, the  
87 optical orientation of the olivine was established, and the optical retardation (i.e., the  
88 wavelength difference between the fast and slow rays) were estimated. The maximum rod  
89 lengths were measured using a calibrated graticule.

90

91 Out of several hundred Fa grains examined, seventeen were identified that contained  
92 clusters of Qtz rods. In each cluster, every rod is exactly parallel with others within the  
93 host Fa, and each rod consists of a single Qtz crystal (Fig. 1). The clusters consistently  
94 have dimensions of ~ 0.1 mm perpendicular to the rod elongation direction, and ~0.3 –  
95 0.4 mm parallel to the rod elongation direction. The maximum rod length that is  
96 measured is ~180  $\mu$  (Fig. 2), which is observed when either the (001) or (010) planes are  
97 parallel to the microscope stage. The minimum elongation of ~15  $\mu$  is observed at a  
98 retardation value very close to that for a crystal viewed along the x-axis (i.e., in the [100]  
99 direction). All Qtz rods in a given cluster go to extinction at the same stage rotation  
100 position, which is also the same extinction position as the host Fa (Fig. 1E, F). Where it is  
101 possible to determine cross sectional morphology of the rods (e.g., Fig. 1D), they are  
102 consistently 4-sided rhombohedra, suggesting crystallographic control imposed by the  
103 host Fa.

104

105 The maximum measured rod length for a given inclination angle relative to the plane of  
106 the thin section can be computed from  $l_i = l \times \sin(\theta)$  where  $l_i$  is the observed length,  $l$  is  
107 the actual length and  $\theta$  is the angle of inclination. Plotted in Figure 2 are the envelopes  
108 for what would be the observed rod lengths if the actual lengths were either 200 $\mu$  or  
109 500 $\mu$ , assuming the rods were parallel to the x-axis. All of the data points fall within the  
110 500 $\mu$  envelope (within analytical uncertainty). These observations require that the Qtz  
111 rods are aligned parallel to the [100] direction in all occurrences, with maximum lengths  
112 of less than 500 $\mu$ .

113

114 Exsolved magnetite (Mag) rods were observed in close proximity to Qtz rods in one Fa  
115 host (Fig. 1A). Given that Mag exsolution occurs in the [010] direction (Zhang et al.,  
116 1999; Franz and Wirth, 2000) and that the observed Mag rods are perpendicular to the  
117 coexisting Qtz rods in a host with modest birefringence, this observation is consistent  
118 with the inference above that the Qtz rods are aligned parallel to the [100] direction. This  
119 alignment is also consistent with the Qtz rods occurring along low energy planes in Fa,  
120 which exhibits parting along {010} and {100}.

121

122 A Leitz four-axis universal stage was also used to obtain orientation data for three  
123 clusters of rods in grains that were suitably located in the thin section to allow end-on  
124 observations of the rods. In this case, the stage was used to orient the thin section such  
125 that the maximum retardation could be estimated when the rods were vertically oriented.  
126 In each case, maximum retardation values of ~1230 nm (+/- 50 nm) were obtained, which  
127 is consistent with rod orientations parallel to [100].

128

129 These results show that the rods are highly elongate prismatic forms, with a maximum  
130 length of <500 $\mu$ . The rods are consistently parallel to the Fa x-axis (i.e., the [100]  
131 direction). All of the Qtz rods in a given cluster have identical crystallographic  
132 orientations and are single crystals. Each cluster occurs in a domain that is ca. 0.1 mm  
133 across and ca. 0.3-0.4 mm long. These observations support the suggestion that the Qtz  
134 rods are exsolution features.

135

136 **Olivine Compositions**

137 Experimental data for the Fe- and Mn-rich portion of the MgO-FeO-MnO-SiO<sub>2</sub> system  
138 that would be relevant for the compositions of minerals in this rock are not available.  
139 However, Akaogi et. al. (1989) examined phase relationships in the entire compositional  
140 range in the MgO-FeO-SiO<sub>2</sub> system under conditions relevant for this sample. Their  
141 experiments indicate that  $\alpha$  and  $\gamma$  phases would have coexisted during the peak UHP  
142 conditions this sample experienced. According to their results, the fayalitic  $\alpha$  phase  
143 would have a slightly higher Mg content than the  $\gamma$  phase with which it coexisted. If it is  
144 postulated that during ahrensite inversion to Fa the Fe:Mg:Mn mole proportions were  
145 preserved, the Fa in proximity to the Qtz rods would be expected to possess a lower Mg  
146 content than olivines preserved from the UHP conditions.

147

148 Three distinct occurrences of olivine can be identified in this sample. Matrix Fa is  
149 common, making up ~35% of the rock volume. Olivine is also observed in pigeonite  
150 (Pgt) grains in bands and multiphase inclusions composed of Fa + Qtz with minor Cpx,  
151 always with the same relative volumetric proportions. We interpret the consistent phase  
152 volume proportions (Fa  $\cong$  Qtz > Cpx) and the occasional idiomorphic form of the  
153 inclusions to indicate that these are the breakdown products of orthoferrosilite (Fs).  
154 Finally, a few olivine inclusions occur in the diamond-bearing mantles of garnets.  
155 Because these olivine inclusions occur in the garnet that is inferred to preserve evidence  
156 of the UHP conditions (Glassley et al., 2014), it is these olivines that would have  
157 coexisted with the  $\gamma$  phase. The compositions for the olivines included in garnets, as well  
158 as the compositions of olivines in the other environments were obtained through electron  
159 microprobe (EMP) analysis and are shown in Figure 3.

160

161 The binary phase loop derived by Akaogi et al (1989), for coexisting  $\alpha$  and  $\gamma$  phases at  
162 the conditions inferred for this sample should differ by  $\sim 2$  mole % Fo (the  $\alpha$  phase being  
163 richer in Fo). The double-headed arrow in Fig. 3 indicates this compositional range. The  
164 Fa inclusions in garnet, which would correspond to the  $\alpha$  phase, are consistently the most  
165 Fo-rich of all olivines observed in this rock (Fig. 3) and are nearly 2 mole % richer in Fo  
166 than the Fa adjacent to the Qtz rods (postulated to be derived from the  $\gamma$  phase). These  
167 compositional characteristics are therefore consistent with that predicted from the  
168 experimental data. However, the high  $\text{Mn}_2\text{SiO}_4$  (tephroite [Tep]) content makes this  
169 comparison with the experimental data somewhat equivocal, given the fact that Mn often  
170 contributes notable non-ideality to mixing models. Even so, the striking correspondence  
171 between experimental data and observations lends support to our suggestion that the Qtz-  
172 rod – bearing olivines in this sample preserve evidence of a precursory ahrensite phase.

173

174 In summary, Qtz rods aligned parallel to [100] exhibit optical properties consistent with  
175 an exsolution origin, i.e., coherent crystallographic alignment within host Fa and with  
176 other rods in a given cluster, and occurrence along a low energy plane. The rods have  
177 width dimensions of  $1\text{-}5\mu$  and likely maximum lengths of  $<500\mu$ , which gives them an  
178 aspect ratio of  $\sim 100$  to 1. The rod clusters define domains of approximately  $0.1 \times 0.3\text{-}0.4$   
179 mm, which would have been the minimum grain size for the  $\gamma$  phase. The Fo : (Fa + Tep)  
180 ratios for Fa inclusions in garnets (remnants from the UHP phase of metamorphism) and  
181 the Fa in proximity to Qtz rods are consistent with that expected for coexisting Fa and  
182 ahrensite, based on experimental data.



183

184 These results provide tentative support for the hypothesis that UHP metamorphism of this  
185 sample resulted in the development of coexisting  $\alpha$  and  $\gamma$  (Fe,Mn)<sub>2</sub>SiO<sub>4</sub> phases (the latter  
186 being somewhat supersilicic). Following peak metamorphic conditions, ascent to  
187 shallower levels led to inversion of the  $\gamma$  phase to Fa, accompanied by exsolution of  
188 excess SiO<sub>2</sub>. The precise conditions at which inversion and exsolution occurred are  
189 difficult to establish, however, because of the unusually high Mn content of these phases,  
190 for which appropriate experimental data and thermodynamic properties are lacking.

191

## 192 **Implications**

193

194 These results imply that other occurrences of inverted  $\gamma$  phase are likely to be present in  
195 UHP regimes in which iron- and manganese-rich lithologies occur. Finding such  
196 occurrences would allow more thorough characterization of subduction systems and  
197 processes, as well as providing concrete observational data useful for constraining mantle  
198 mineralogy. Additionally, the absence of adequate experimental data for the Fe-Mg-Mn-  
199 SiO<sub>2</sub> to characterize UHP mineral assemblages points to the need for an experimental  
200 program that would address this deficiency.

201

## 202 **ACKNOWLEDGEMENTS**

203

204 We thank Jane Selverstone for useful comments on an earlier version of this document.

205 We also thank Howard Day and Robert Zierenberg for resurrecting the universal stage.

206 Reviews by W.L. Griffin, J.G. Liou, I.P. Swainson and an anonymous reviewer greatly  
207 improved the manuscript and are gratefully acknowledged.

208

209 **REFERENCES**

210

211 Akaogi, M., and Akimoto, S. (1979) High-pressure phase equilibria in a garnet  
212 lherzolite, with special reference to Mg<sup>2+</sup>-Fe<sup>2+</sup> partitioning among constituent  
213 phases. *Physics of the Earth and Planetary Interiors*, 19, 31–51.

214

215 Akaogi, M., Ito, E. and Navrotsky, A. (1989) Olivine-modified spinel-spinel transitions  
216 in the system Mg<sub>2</sub>SiO<sub>4</sub>-Fe<sub>2</sub>SiO<sub>4</sub>: Calorimetric measurements, thermochemical calculation  
217 and geophysical application. *Journal of Geophysical Research*, 94, 15,671-15,685.

218

219 Day, H., and Mulcahy, S.R. (2007) Excess silica in omphacite and the formation of  
220 free silica in eclogite. *Journal of Metamorphic Geology*, 25, 37–50.

221

222 Feng, L., Lin, Y., Hu, S., Xu, L. and Miao, B. (2011) Estimating compositions of natural  
223 ringwoodite in the heavily shocked Grove Mountains 052049 meteorite from Raman  
224 spectra. *American Mineralogist* 96, 1480-1489.

225

226 Franz, L. and Wirth, R. (2000) Spinel inclusions in olivine of peridotite xenoliths from  
227 TUBAF seamount (Bismarck Archipelago/Papua New Guinea): evidence for the thermal

228 and tectonic evolution of the oceanic lithosphere. Contributions to Mineralogy and  
229 Petrology 140, 283-295.

230

231 Glassley, W.E., Korstgård, J.A., Sørensen, K. and Platou, S. (2014) A new UHP  
232 metamorphic complex in the ~1.8 Ga Nagssugtoqidian Orogen of West Greenland.  
233 American Mineralogist, 99, 1315-1344.

234

235 Hazen, R.M., Downs, R.T., Finger, L.W., and Ko, J. (1993) Crystal chemistry of  
236 ferromagnesian silicate spinels: Evidence for Mg-Si disorder. American Mineralogist, 78,  
237 1320-1323.

238

239 Irifune, T., and Ringwood, A.E. (1987) Phase transformations in a harzburgite  
240 composition to 26 GPa: implications for dynamical behaviour of the subducting slab.  
241 Earth and Planetary Science Letters, 86, 365-376.

242

243 Ma, C., Tschauner, O., Liu, Y., Beckett, J.R., Rossman, G.R., Zurelev, K., Prakapenka,  
244 V., Dera., P., Sinogeikin, S., Smith, J. and Taylor, L. (2014) Discovery of  $\gamma$ -Fe<sub>2</sub>SiO<sub>4</sub> and  
245 tissintite (Ca,Na,~)AlSi<sub>2</sub>O<sub>6</sub>: Two new high pressure minerals from the Tissint Martian  
246 meteorite. 45<sup>th</sup> Lunar and Planetary Science Conference, 3 p.

247

248 Ma, C., Tschauner, O., Beckett, J.R., Liu, Y., Rossman, G.R., Sinogeikin, S., V., Smith,  
249 J. and Taylor, L.A. (2016) Ahrensite,  $\gamma$ -Fe<sub>2</sub>SiO<sub>4</sub>, a new shock-metamorphic mineral

250 from the Tissint meteorite: Implications for the Tissint shock event on Mars. *Geochimica*  
251 *et Cosmochimica Acta*, 184, 240-256.

252

253 Xie, Z., Tomioka, N. and Sharp, T.G. (2002) Natural occurrence of Fe<sub>2</sub>SiO<sub>4</sub>-spinel in the  
254 shocked Umbarger L6 chondrite. *American Mineralogist* 87, 1257-1260.

255

256 Zhang, R.Y., Shu, J.F., Mao, H.K. and Liou, J.G. (1999) Magnetite lamellae in olivine  
257 and clinohumite from Dabie UHP ultramafic rocks, central China. *American Mineralogist*  
258 84, 564-569.

259

260

## 261 **Figure Captions**

262

263 Figure 1. Two examples of Qtz lamellae in Fa. A. Cross-nicols view of Mag exsolution  
264 and Qtz rods (both indicated by arrows) in Fa (area L6). The orientation of the (010) and  
265 (100) planes is shown. B-F. Transmitted (B., E. and F.) and reflected (C. and D.) light  
266 images of area H10 at different magnifications. Qtz rods are the parallel dark lineations.  
267 The arrow in D. indicates an obvious prismatic form of a Qtz rod very slightly inclined to  
268 the plane of the thin section. E. shows the Fa crystal at extinction (shadow enhanced)  
269 with the Qtz rods also uniformly at extinction. Note the slight strain in the Fa crystal,  
270 which accounts for the very slight, irregular birefringence. F. shows the area in E. (boxed  
271 region), rotated to show maximum birefringence. The green arrow points to the same  
272 location on one of the Qtz rods, for reference.

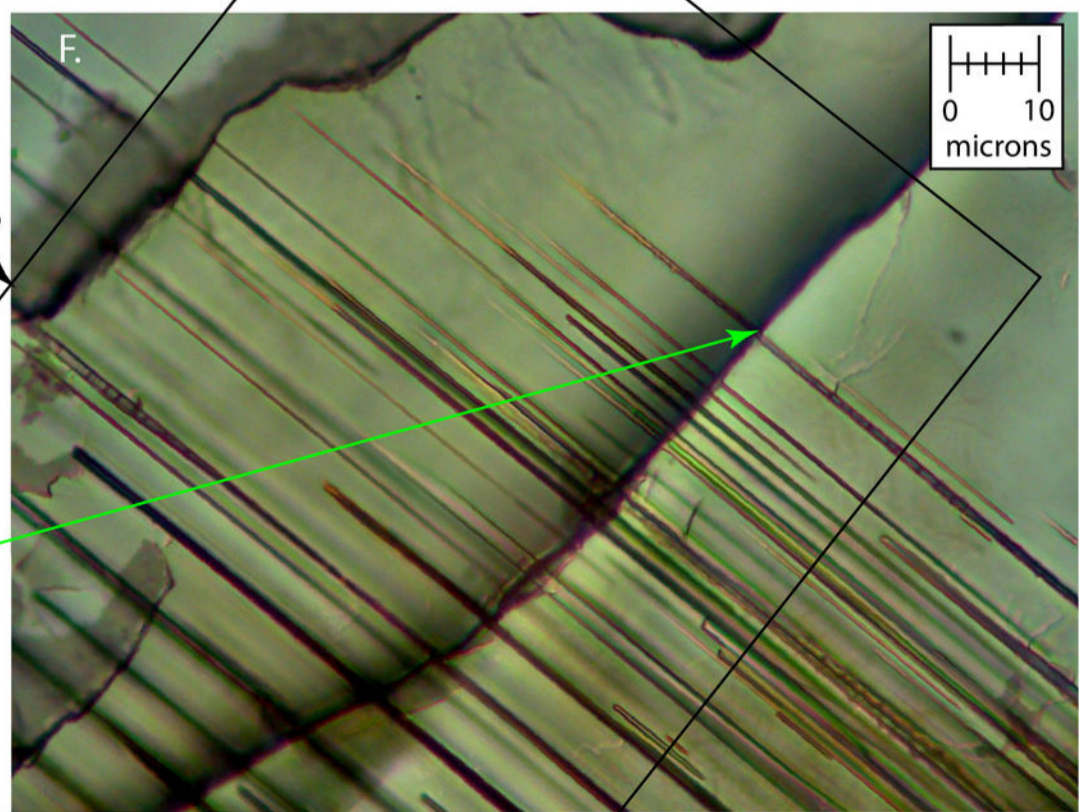
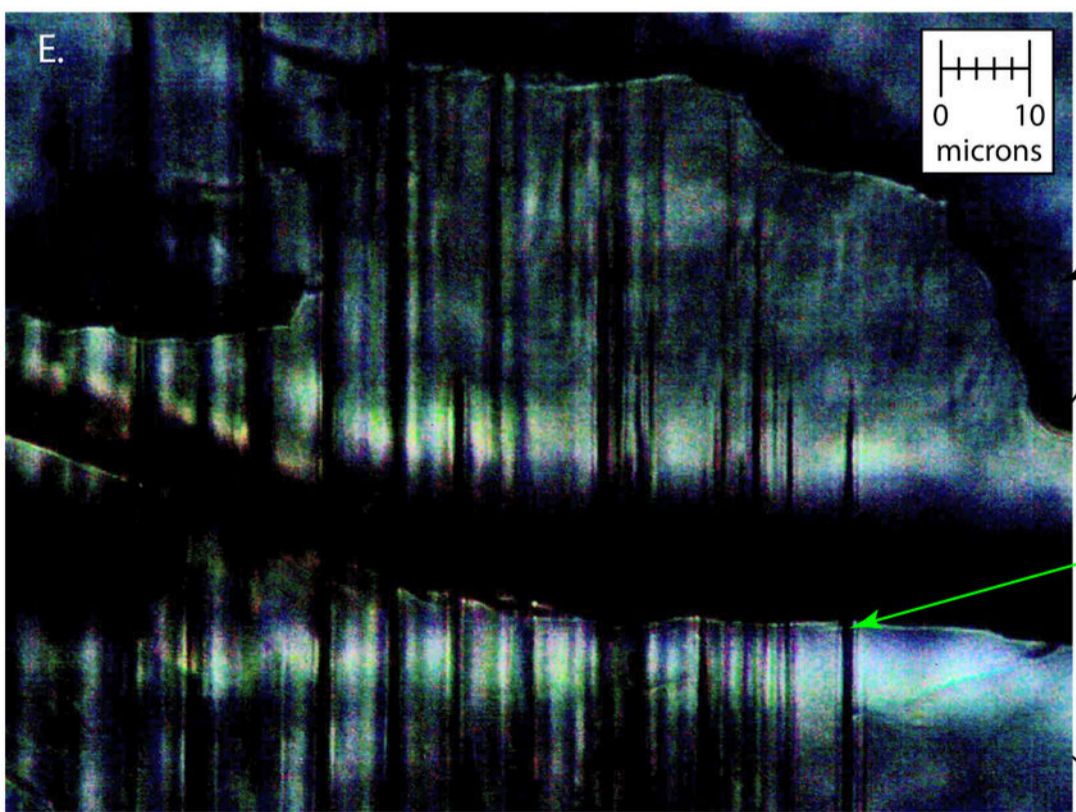
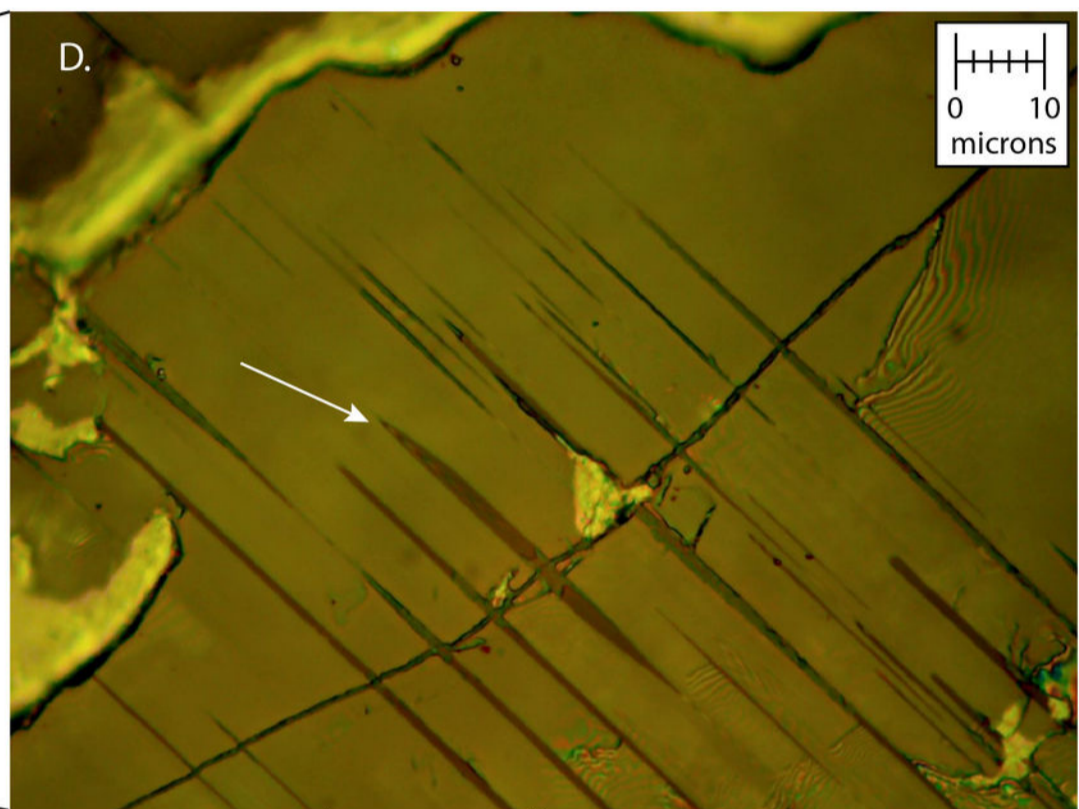
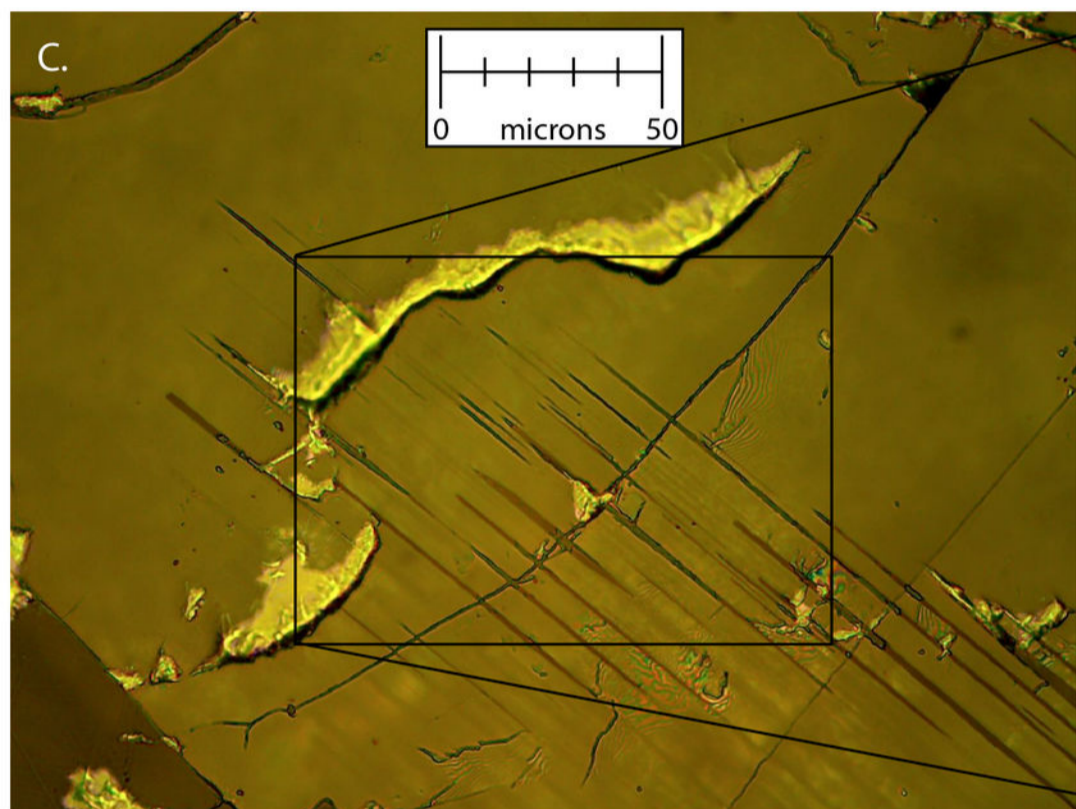
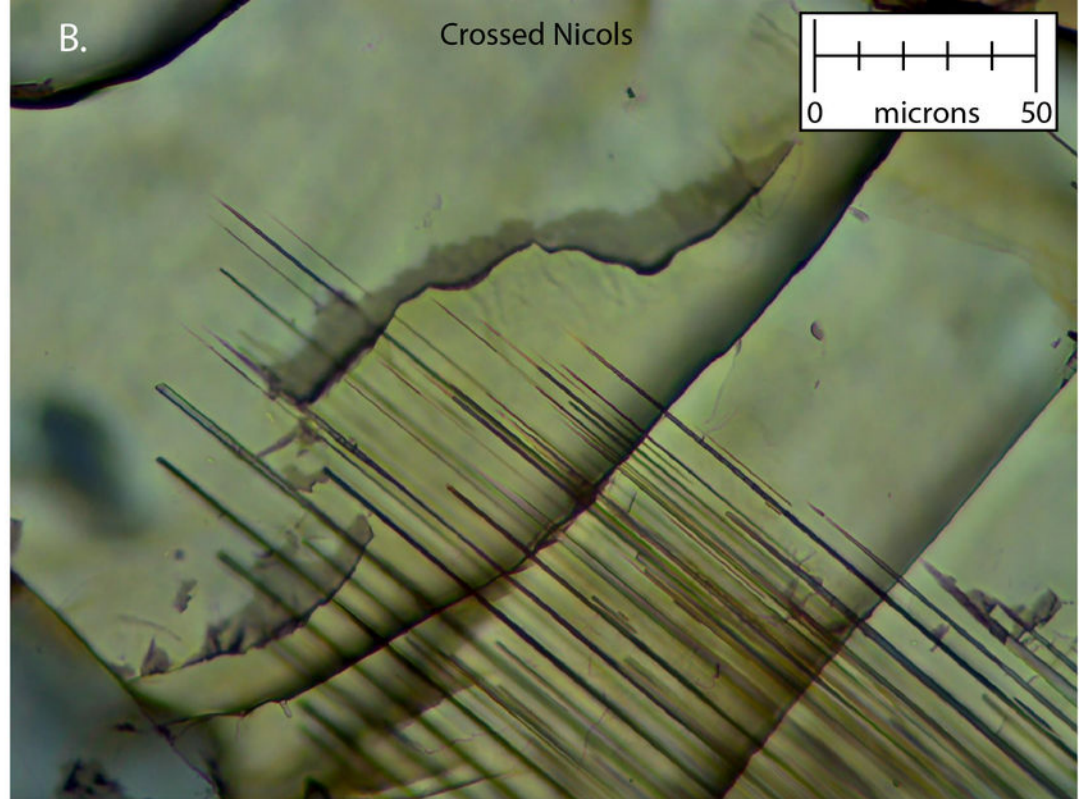
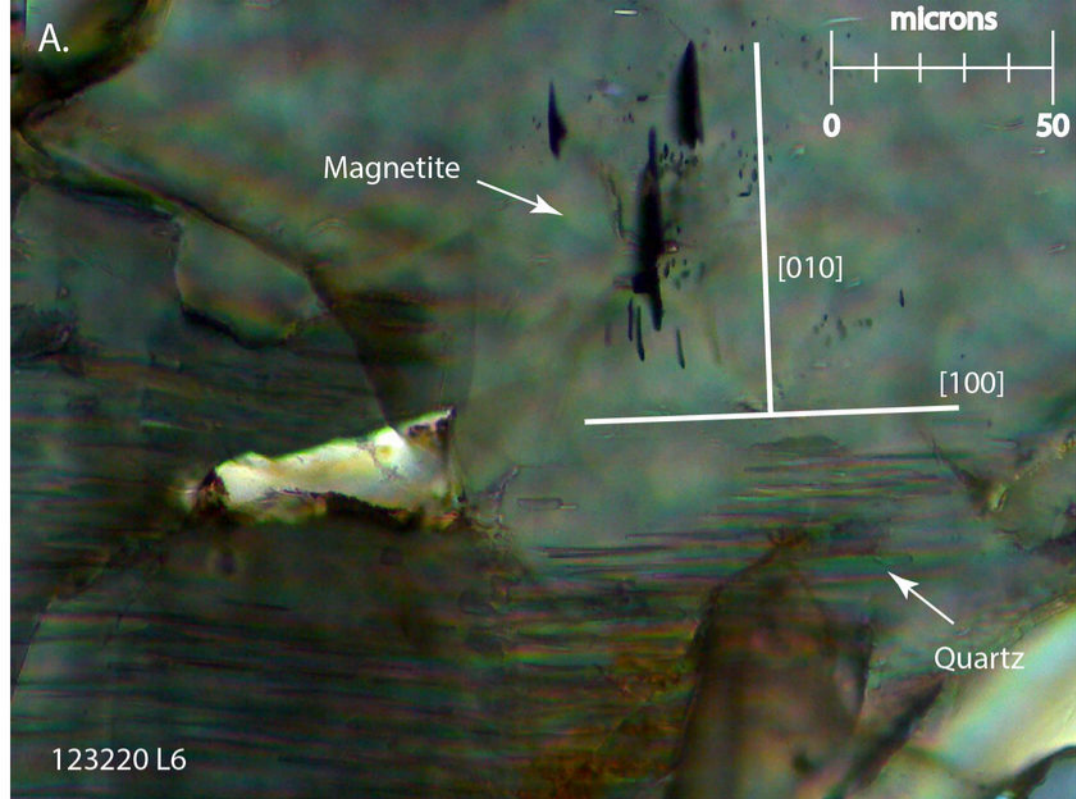
273

274 Figure 2. Graph of maximum measured rod length (in microns) vs estimated optical  
275 retardation (in nanometers). The vertical bars indicate the optical retardation that would  
276 be expected for Fa when viewed along the indicated directions. The dashed lines are  
277 calculated envelopes of rod lengths that would be observed for rods inclined to the plane  
278 of the thin section, assuming maximum rod lengths of  $200\mu$  (long dashed lines) and  $500\mu$   
279 (short dashed, arrowed lines) and the rods are elongate parallel to the x axis.

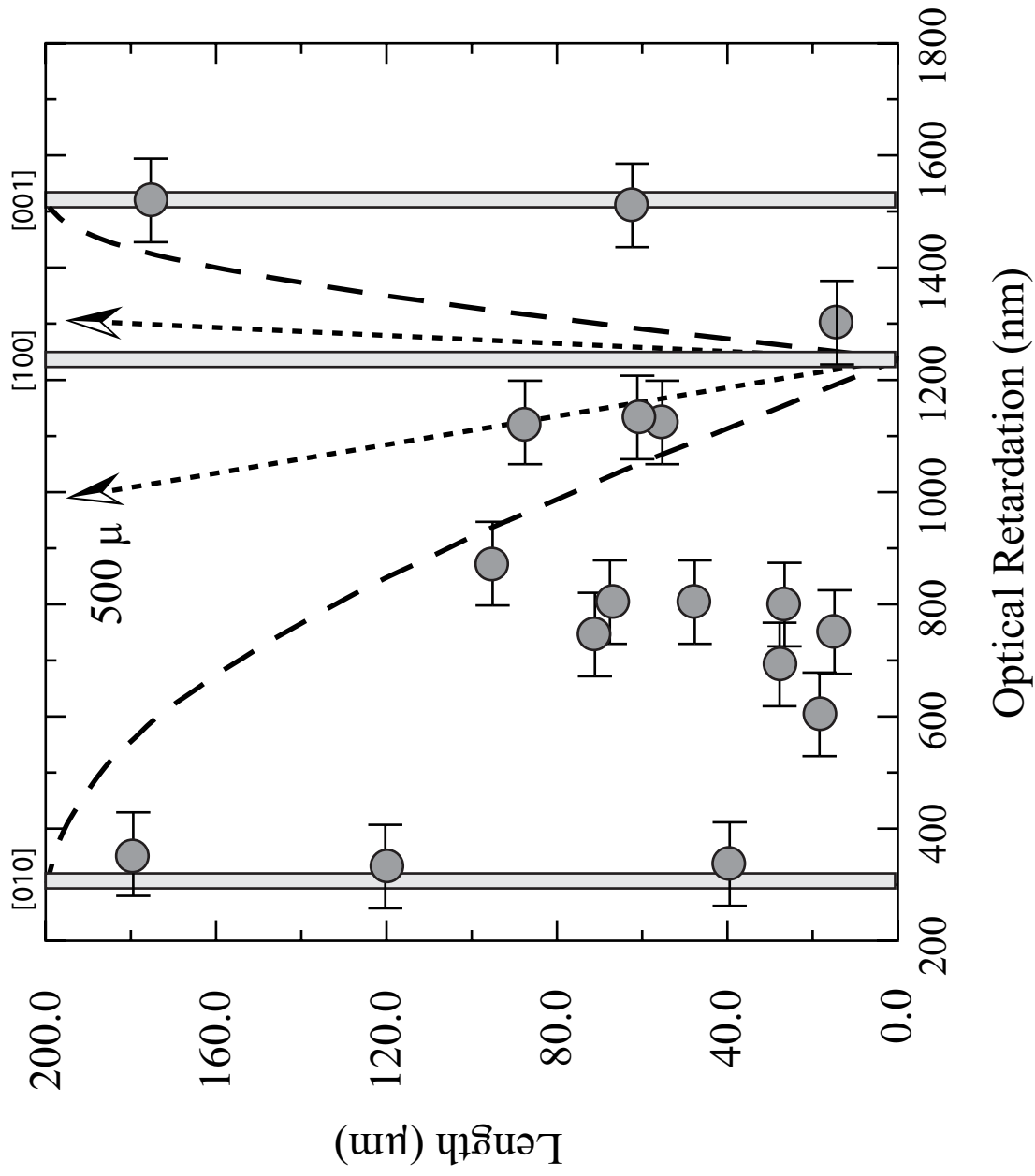
280

281 Figure 3. Histogram of number of olivine analyses with Mg atoms per formula unit  
282 (assuming 4 oxygens; bin size of 0.001). Analyses from inclusions of olivine in garnet  
283 zones containing relict diamond are blue (Fa in garnet). Also shown are analyses for  
284 olivines in immediate vicinity of Qtz lamellae (Fa in proximity to quartz lamellae; black),  
285 matrix olivines (Fa in matrix; orange), olivines that formed during inversion of ferrosilite  
286 (Fa after Fs; green), and matrix olivines in contact with garnet (Matrix Fa adjacent to  
287 garnet; gray). The mean values for each Fa group are shown by the color-filled squares.  
288 The horizontal bar running through each square is the standard deviation, based on EMP  
289 analytical statistics. The heavy horizontal arrows show expected Fa compositions, as  
290 explained in the text.

291



123220 H10



Glassley et al, Ahrensite

Figure 2

